

CrossMark
click for updatesCite this: *Chem. Sci.*, 2016, 7, 4980

Received 29th March 2016

Accepted 10th May 2016

DOI: 10.1039/c6sc01376g

www.rsc.org/chemicalscience

A metal–organic framework immobilised iridium pincer complex†

Martino Rimoldi,^a Akitake Nakamura,^a Nicolaas A. Vermeulen,^a James J. Henkelis,^a Anthea K. Blackburn,^a Joseph T. Hupp,^a J. Fraser Stoddart^{*a} and Omar K. Farha^{*ab}

An iridium pincer complex has been immobilised in the metal–organic framework **NU-1000** using a technique called solvent assisted ligand-incorporation (SALI). The framework proved to be stable under the conditions required to activate the iridium complex and spectroscopic investigations showed formation of the catalytically active iridium dihydride. The Ir-pincer modified **NU-1000** is an active catalyst for the condensed phase hydrogenation of a liquid alkene (1-decene and styrene) and shows enhanced activity with respect to a homogeneous analogue. Additionally, the Ir-pincer immobilised inside **NU-1000** operated as an efficient heterogeneous catalyst under flow conditions.

Introduction

Pincer complexes have been widely used and investigated for application in homogeneous catalytic transformations.¹ Iridium pincer complexes are of special interest and were first prepared two decades ago.² Their chemistry is still the object of numerous investigations³ and this class of complexes are extremely effective in applications involving hydrocarbon conversions.⁴ Heterogenisation of organometallic complexes has been under extensive study, especially employing amorphous metal oxides as supports.⁵

Generally, supporting an organometallic species requires the use of organic ligands designed to enable anchoring on a heterogeneous substrate.⁶ The ligands are often complex and require a significant investment in synthesis. This approach aims to yield single sites or usually well-defined systems, whose characterisation is not always straightforward.

Recently this approach has also been applied to the post-synthetic metalation of MOFs to afford, amongst others, Co(II)- and Fe(II)-based single-site catalysts that were found active in various transformations. In particular, high turnover numbers were obtained in alkene hydrogenations. Catalytic tests were typically conducted at 40 bar, room temperature and using THF as solvent.⁷

To date, only a few heterogeneous materials containing pincer complexes have been prepared and used in catalytic processes.⁸

Herein, we describe the incorporation of a catalytically active iridium pincer complex into a metal–organic framework (MOF). We selected **NU-1000**⁹ – a mesoporous MOF (Fig. 1) featuring 30 Å channels with Zr₆ oxide metal nodes and 1,3,6,8-tetrakis(*p*-benzoic acid)pyrene as the tetratopic linkers—as the heterogenization platform. Detailed physical and structural characterisations, as well as the elucidation of the proton topology around the node, have been described^{9,10} recently and a post-synthetic modification, called solvent assisted ligand-incorporation¹¹ (SALI) has been used to decorate the metal nodes of **NU-1000** with carboxylic acid containing molecules. SALI makes use of carboxyl groups to displace labile –OH and H₂O ligands on the Zr₆ node and form strong chelating metal–ligand bond. In this report, an Ir(III) complex featuring a bis-phosphinite pincer ligand, similar to those introduced and developed by Brookhart and co-workers,¹² has been incorporated into **NU-1000** using SALI and its catalytic activity tested in a hydrogenation reaction.

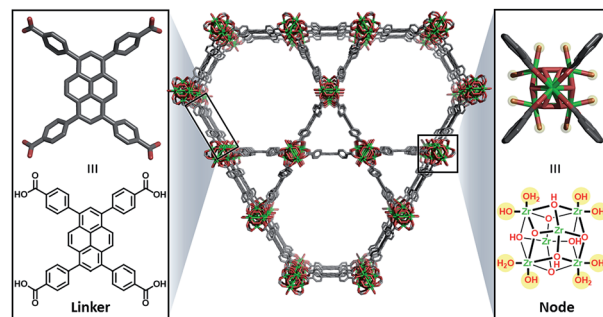


Fig. 1 Unfunctionalised **NU-1000** showing the linker (left) and node (right) with the displaceable –OH and H₂O ligands highlighted in yellow.

^aDepartment of Chemistry, Northwestern University, 2145 Sheridan Road, Evanston, Illinois 60208, USA. E-mail: jfstoddart@gmail.com; omarfharha@gmail.com

^bDepartment of Chemistry, Faculty of Science, King Abdulaziz University, Jeddah, Saudi Arabia

† Electronic supplementary information (ESI) available: Detailed experimental procedures. CCDC 1465323. For ESI and crystallographic data in CIF or other electronic format see DOI: 10.1039/c6sc01376g

Results and discussion

The synthetic route outlined in Scheme 1 was used to prepare the carboxylic acid functionalised pincer complex **3**. Firstly, the TBDMS-protected bis-phosphinite ligand (see ESI†) was reacted with $[\text{IrCl}(\text{COD})]_2$ to afford the complex **1**. Deprotection of the phenol silyl ether using $\text{Cu}(\text{II})$ chloride led to the formation of the phenolic derivative **2** as the major product. At this stage we observed that one of the *tert*-butyl phosphinite substituents had reacted with the metal center to form a cyclometallated four-membered ring compound **2**. Similar complexes have been reported¹³ and their distinctive characterisation data described. The ^{31}P NMR spectrum of **2** (and of the complexes obtained in the subsequent steps) shows a set of resonances (two doublets) at δ 160.4 and 119.3, confirming the asymmetry of the complex and the existence of two heterotopic phosphorous atoms. Notably, the hydride signal (δ –41.9) that characterises the complex **1** is no longer observed. Single crystal X-ray diffraction analysis confirms (Fig. 2) the structural assignment of **2**.

Etherification, using methyl chloroacetate and subsequent hydrolysis completes the synthesis of the desired carboxylic acid functionalised pincer complex **3**. Hydride iridium pincer complexes are known¹⁴ to activate a variety of unreactive bonds and to prevent the pincer complex from reacting in an uncontrolled fashion with the zirconium nodes or with the organic linkers in the MOF, we decided to perform SALI with the iridium–chloride complex **3** and to proceed to its activation in a subsequent step.¹⁵

NU-1000 was suspended in a PhMe solution of **3** and allowed to react at room temperature (see ESI†). After 24 h, the MOF changed colour from yellow to orange, indicating (Scheme 2) the incorporation of the iridium complex and the formation of **4**. The solid was thoroughly washed¹⁶ with PhMe. Inductively coupled plasma – optical emission spectrometry (ICP-OES) of **4** showed an Ir : P : Zr ratio of 0.8 : 1.5 : 6 (in theory a 1 : 2 : 6 ratio is expected for incorporation of one iridium pincer complex per node) and confirmed the incorporation of the iridium complex into the framework with a loading of

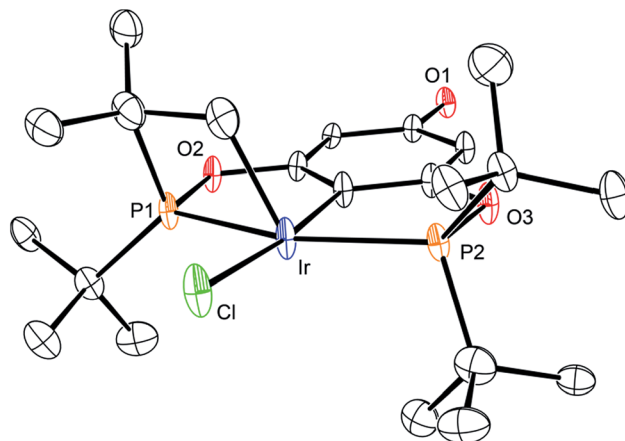
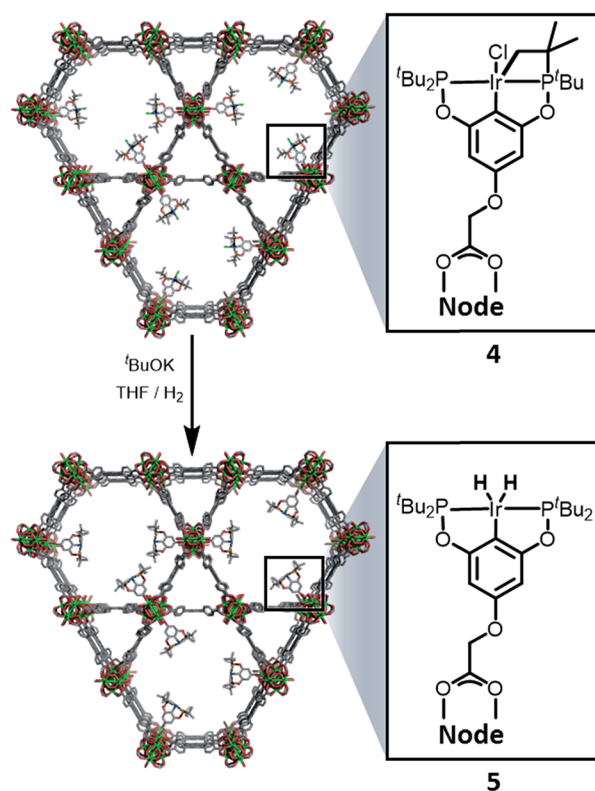
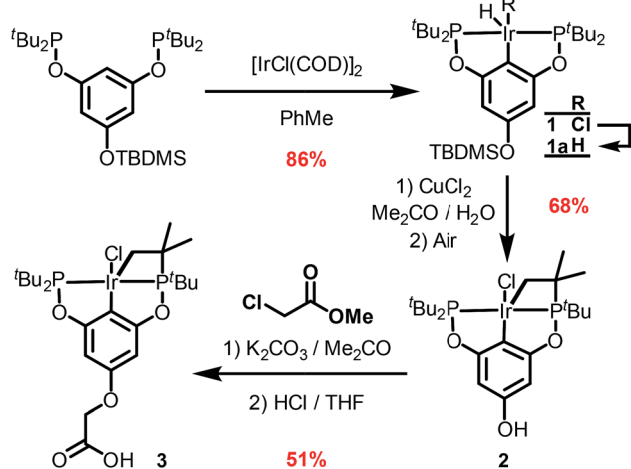


Fig. 2 ORTEP drawing of **2**. Hydrogen atoms are omitted for clarity, and thermal ellipsoids are set to 20% probability. Only one set of disordered *tert*-butyl groups and chlorides are shown for clarity.



Scheme 2 Reactivity of **4** with $t\text{BuOK}$ and H_2 to give the NU-1000 supported dihydride iridium pincer complex, **5**.



Scheme 1 Synthesis of the complex **3**.

0.8 iridium complexes per Zr_6 node. Scanning electron microscopy-energy dispersive X-ray spectroscopy (SEM-EDS) confirms that following SALI, crystallites of NU-1000 retain their morphology while the iridium complex is evenly distributed (see ESI†) within the crystal. The identity of the heterogenised complex was probed by solid-state ^{31}P MAS NMR spectroscopy. A set of two signals at δ 158 and 116 was observed, in good agreement with those found (δ 160.9 and 119.5 see Fig. 3) for the

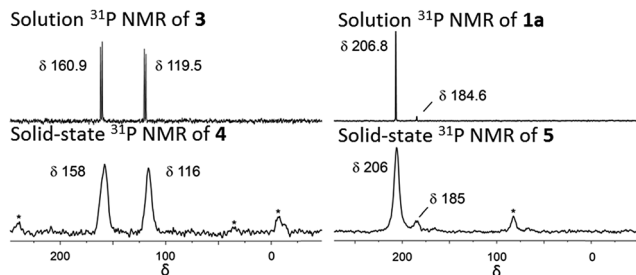


Fig. 3 Solution phase ^{31}P NMR of **3** and **1a** in C_6D_6 at 243 MHz. Solid-state ^{31}P MAS NMR of **4** and **5** at 162 MHz. Asterisks denote spinning side bands.

homogenous starting material **3**. This spectroscopic evidence proves that the pincer complexes remain intact following SALI. Employing procedures previously reported¹² for the activation of homogenous iridium pincer complexes, **4** was exposed to $t\text{BuOK}$ in THF under an atmosphere of H_2 at room temperature (see ESI†). Adoption of this procedure (Scheme 2) allowed us to (i) activate the supported iridium chloride complex^{17,18} and (ii) form the corresponding metal hydride **5**.

Solid-state ^{31}P MAS NMR spectroscopy (Fig. 3) revealed that treatment of **4** with $t\text{BuOK}$ and H_2 produces a material with resonances at δ 206 and 185. These signals correspond¹⁸ to the dihydride complex (δ 206, major) and the tetrahydride complex (δ 185, minor). Additionally, infrared spectroscopy revealed (see ESI†) the appearance of a band at 2006 cm^{-1} in good agreement with the formation of a metal hydride. In addition, powder X-ray diffraction of **4** confirmed the retention of crystallinity following SALI and, more importantly, demonstrated that the framework's extended structure is maintained even after the activation step with $t\text{BuOK}$ to give **5** (see ESI†). Moreover, the porosity of **5** was retained as shown in Fig. S2–3.†

For comparison, we prepared (Scheme 1) the homogeneous dihydride **1a** (see ESI†) from **1**. Solution and solid-state ^{31}P MAS NMR spectra showed (Fig. 3) similar resonances for **1a** and **5**, confirming the presence of analogous Ir(III) complexes in both a homogeneous solution and a heterogeneous material.

Condensed-phase hydrogenation of 1-decene and styrene, catalysed by **1a** and **5** at 1 bar (abs.) and 23°C , were used to examine the relative catalytic activities of the homogenous and heterogeneous Ir(III) catalysts (see ESI†). With 1-decene as the substrate, turnover frequencies (TOFs) of 0.3 and 2.3 h^{-1} for **1a** and **5**, respectively, were calculated. Catalysis with styrene reveals TOFs of 0.1 and 7.2 h^{-1} in the case of **1a** and **5**, respectively. In both examples, **5** proved (Fig. 4) to be more active than the homogeneous catalyst **1a**.

Leaching tests on the heterogeneously catalysed reactions showed that the liquid phase is not catalytically active, confirming that the Ir(III) pincer complex is not released into the solution.

Although a thorough explanation of such enhanced activity is not trivial, we speculate that site isolation caused by the hetero-organization of the molecular complex reduces intermolecular interactions that could deactivate the catalyst or interfere in the catalytic cycle. Similar behaviour has recently been reported.^{8f,19}

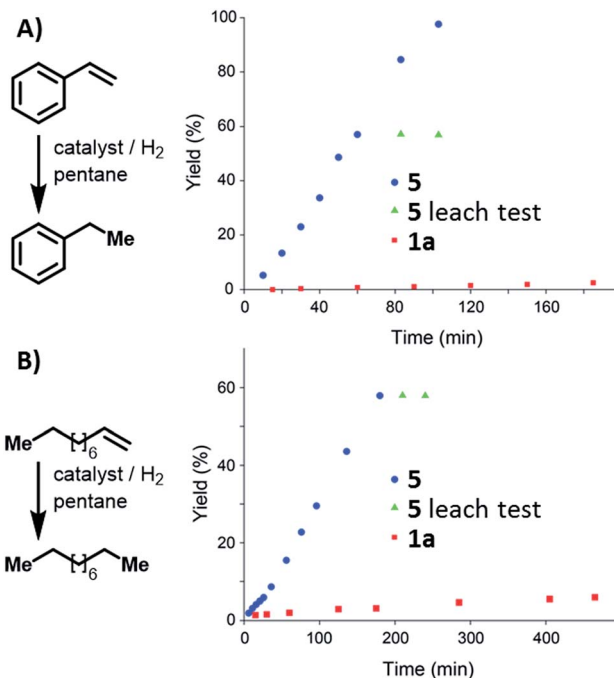


Fig. 4 Reaction profile of styrene (A) and 1-decene (B) hydrogenation catalysed by **1a**, and **5**. Leaching tests performed using **5** indicate that the solution did not contain active catalyst.

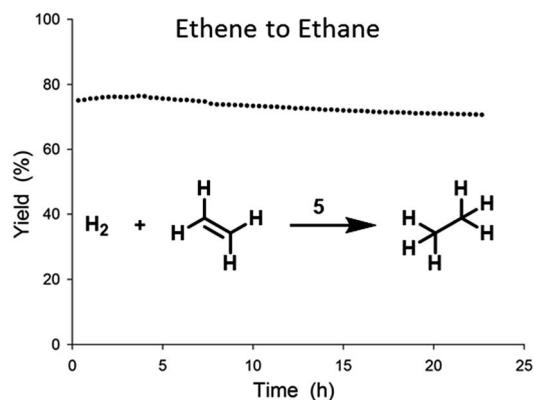


Fig. 5 Stability test of ethene hydrogenation catalysed by **5** in flow reactor at 0.5 bar (rel.) and at 23°C , with an ethene : hydrogen ratio of 1 : 1 and a total flow of 80 mL min^{-1} .

In order to probe the activity of catalyst **5**, we tested gas-phase ethene hydrogenation in a tubular flow reactor. The TOF was determined under differential conditions at conversions below 5% (see ESI†). Catalyst **5** showed a TOF value of 0.32 s^{-1} at 50°C , 1 bar (rel.), and with an ethene : hydrogen ratio of 1 : 1.²⁰ Little deactivation was observed over time and stability tests (Fig. 5) showed only minor losses (4%) of activity over the course of 24 h.

Conclusions

We report attaching an iridium pincer complex inside a MOF without having to synthesise the extended structure *de novo*.



The complex can be activated after its incorporation to yield the active dihydrido-iridium catalyst. Despite the basic conditions required to carry out the chloride-abstraction, the crystallinity and porosity of the framework are retained and spectroscopic investigations corroborate the similarity between the solid and the related homogeneous catalyst. This observation establishes that the catalytically active site characteristic of the molecular compound has been preserved upon its heterogenization. In order to demonstrate the accessibility to the active sites, we tested this material in the hydrogenation of liquid substrates and with ethene (gas) under flow conditions – the latter being possible only with the catalyst in heterogeneous form. It is noteworthy that the heterogeneous catalyst shows enhanced activity with respect to its homogeneous counterpart and reveals stability upon prolonged use. This work serves as a proof-of-concept that well studied organometallic complexes can be installed and activated within a crystalline metal–organic framework.

Acknowledgements

This work was supported as part of the Inorganometallic Catalyst Design Center, an Energy Frontier Research Center funded by the U.S. Department of Energy (DOE), Office of Science, Basic Energy Sciences (BES), under award DE-SC0012702. This research is part of the Joint Center of Excellence in Integrated Nano-Systems (JCIN) at King Abdulaziz City for Science and Technology (KACST) at Northwestern University (NU). The authors would like to thank both KACST and NU for their continued support of this research which made use of the IMSERC facility supported by the National Science Foundation (NSF, DMR-0521267); the J.B.Cohen X-Ray Diffraction Facility at the Materials Research Center of NU supported by the MRSEC (NSF, DMR-1121262); the EPIC facility of the NUANCE Center at NU, which has received support from the Soft and Hybrid Nanotechnology Experimental (SHyNE) Resource (NSF, NNCI-1542205); the International Institute for Nanotechnology (IIN); the Keck Foundation; and the State of Illinois, through the IIN. Metal analysis was performed at the NU Quantitative Bioelement Imaging Center. M.R. was supported by the Swiss National Science Foundation with an “Early Postdoc Mobility Fellowship”. A.K.B. thanks Fulbright New Zealand for a Fulbright Graduate Award and the New Zealand Federation of Graduate Women for a Postgraduate Fellowship Award.

Notes and references

- (a) R. Langer, Y. Diskin-Posner, G. Leitus, L. J. W. Shimon, Y. Ben-David and D. Milstein, *Angew. Chem., Int. Ed.*, 2011, **50**, 9948–9952; (b) N. Selander and K. J. Szabó, *Chem. Rev.*, 2011, **111**, 2048–2076; (c) R. Tanaka, M. Yamashita and K. Nozaki, *J. Am. Chem. Soc.*, 2009, **131**, 14168–14169; (d) P. Kang, C. Cheng, Z. Chen, C. K. Schauer, T. J. Meyer and M. Brookhart, *J. Am. Chem. Soc.*, 2012, **134**, 5500–5503; (e) C.-I. Lee, J. Zhou and O. V. Ozerov, *J. Am. Chem. Soc.*, 2013, **135**, 3560–3566.
- (a) M. Gupta, C. Hagen, W. C. Kaska, R. E. Cramer and C. M. Jensen, *J. Am. Chem. Soc.*, 1997, **119**, 840–841; (b) C. J. Moulton and B. L. Shaw, *J. Chem. Soc., Dalton Trans.*, 1976, 1020–1024.
- M. C. Haibach, S. Kundu, M. Brookhart and A. S. Goldman, *Acc. Chem. Res.*, 2012, **45**, 947–958.
- (a) A. S. Goldman, A. H. Roy, Z. Huang, R. Ahuja, W. Schinski and M. Brookhart, *Science*, 2006, **312**, 257–261; (b) R. Ahuja, B. Punji, M. Findlater, C. Supplee, W. Schinski, M. Brookhart and A. S. Goldman, *Nat. Chem.*, 2011, **3**, 167–171.
- J. M. Thomas, *Design and Application of Single-Site Heterogeneous Catalysts*, Imperial College Press, London, 2012.
- G. Ertl, H. Knözinger, F. Schüth and J. Weitkamp, *Handbook of Heterogeneous Catalysis*, Wiley-VCH, Weinheim, 2008.
- (a) K. Manna, T. Zhang, M. Carboni, C. W. Abney and W. Lin, *J. Am. Chem. Soc.*, 2014, **136**, 13182–13185; (b) T. Zhang, K. Manna and W. Lin, *J. Am. Chem. Soc.*, 2016, **138**, 3241–3249; (c) N. C. Thacker, Z. Lin, T. Zhang, J. C. Gilhula, C. W. Abney and W. Lin, *J. Am. Chem. Soc.*, 2016, **138**, 3501–3509.
- (a) Z. Huang, M. Brookhart, A. S. Goldman, S. Kundu, A. Ray, S. L. Scott and B. C. Vicente, *Adv. Synth. Catal.*, 2009, **351**, 188–206; (b) J. Ternel, L. Delevoye, F. Agbossou-Niedercorn, T. Roisnel, R. M. Gauvin and C. M. Thomas, *Dalton Trans.*, 2010, **39**, 3802–3804; (c) E. K. Huang, W. M. Cheung, K. W. Chan, F. L. Y. Lam, X. J. Hu, Q. F. Zhang, I. D. Williams and W. H. Leung, *Eur. J. Inorg. Chem.*, 2013, **2013**, 2893–2899; (d) M. Rimoldi, D. Fodor, J. A. van Bokhoven and A. Mezzetti, *Chem. Commun.*, 2013, **49**, 11314–11316; (e) M. Rimoldi and A. Mezzetti, *Inorg. Chem.*, 2014, **53**, 11974–11984; (f) S. A. Burgess, A. Kassie, S. A. Baranowski, K. J. Fritzscheing, K. Schmidt-Rohr, C. M. Brown and C. R. Wade, *J. Am. Chem. Soc.*, 2016, **138**, 1780–1783.
- J. E. Mondloch, W. Bury, D. Fairen-Jimenez, S. Kwon, E. J. DeMarco, M. H. Weston, A. A. Sarjeant, S. T. Nguyen, P. C. Stair, R. Q. Snurr, O. K. Farha and J. T. Hupp, *J. Am. Chem. Soc.*, 2013, **135**, 10294–10297.
- N. Planas, J. E. Mondloch, S. Tussupbayev, J. Borycz, L. Gagliardi, J. T. Hupp, O. K. Farha and C. J. Cramer, *J. Phys. Chem. Lett.*, 2014, **5**, 3716–3723.
- (a) P. Deria, J. E. Mondloch, E. Tylianakis, P. Ghosh, W. Bury, R. Q. Snurr, J. T. Hupp and O. K. Farha, *J. Am. Chem. Soc.*, 2013, **135**, 16801–16804; (b) P. Deria, Y. G. Chung, R. Q. Snurr, J. T. Hupp and O. K. Farha, *Chem. Sci.*, 2015, **6**, 5172–5176; (c) S. T. Madrahimov, J. R. Gallagher, G. Zhang, Z. Meinhart, S. J. Garibay, M. Delferro, J. T. Miller, O. K. Farha, J. T. Hupp and S. T. Nguyen, *ACS Catal.*, 2015, **5**, 6713–6718.
- I. Gottker-Schnetmann, P. White and M. Brookhart, *J. Am. Chem. Soc.*, 2004, **126**, 1804–1811.
- (a) A. V. Polukeev, S. A. Kuklin, P. V. Petrovskii, A. S. Peregodov, F. M. Dolgushin, M. G. Ezernitskaya and A. A. Koridze, *Russ. Chem. Bull.*, 2010, **59**, 745–749; (b) H. A. Y. Mohammad, J. C. Grimm, K. Eichele, H.-G. Mack,



- B. Speiser, F. Novak, M. G. Quintanilla, W. C. Kaska and H. A. Mayer, *Organometallics*, 2002, **21**, 5775–5784.
- 14 (a) A. C. Sykes, P. White and M. Brookhart, *Organometallics*, 2006, **25**, 1664–1675; (b) I. Gottker-Schnetmann and M. Brookhart, *J. Am. Chem. Soc.*, 2004, **126**, 9330–9338.
- 15 To obtain an active species, iridium-chloride pincer complexes are commonly activated in solution by halogen abstraction under hydrogen atmosphere. This procedure usually affords the corresponding highly reactive dihydride species.
- 16 The remaining reaction solution was shown by ^{31}P NMR to contain exclusively unreacted starting material.
- 17 Phosphinite iridium hydride pincer complexes are known to be stable in the form of dihydride and to loosely coordinate an additional dihydrogen molecule when exposed to hydrogen.
- 18 I. Gottker-Schnetmann, P. S. White and M. Brookhart, *Organometallics*, 2004, **23**, 1766–1776.
- 19 M. Rimoldi, D. Fodor, J. A. van Bokhoven and A. Mezzetti, *Catal. Sci. Technol.*, 2015, **5**, 4574–4586.
- 20 A TOF of 0.14 s^{-1} was obtained at $23\text{ }^{\circ}\text{C}$ and 0.5 bar (rel.).

